

# Crystal Morphology and Phase Identification in Poly(Aryl Ether Ketone)s and Their Copolymers. 4. Morphological Observations in PEKK with All *p*-Phenylene Linkages

Rong-Ming Ho and Stephen Z. D. Cheng\*

Maurice Morton Institute and Department of Polymer Science, The University of Akron, Akron, Ohio 44325-3909

Benjamin S. Hsiao and Kennecorwin H. Gardner

Central Research and Development Department, Experimental Station, E. I. du Pont de Nemours and Company, Wilmington, Delaware 19880-0356

Received May 19, 1995; Revised Manuscript Received September 29, 1995\*

**ABSTRACT:** The thin film crystalline morphology of poly(aryl ether ketone ketone) having all *p*-phenylene linkages [PEKK(T)] has been investigated *via* transmission electron microscopy (TEM) and electron diffraction (ED) experiments. PEKK(T) samples isothermally crystallized from both the melt and the quenched glassy state over a temperature range of 160–360 °C have been examined, and two polymorphs (form I and form II) have been found. At low supercoolings, micrometer-size faceted single lamellar crystals can be found either from the melt or from the glassy state for both forms I and II. On the basis of ED results obtained from the single lamellar crystals, the *c*-axis in both forms is not perpendicular to the substrate. This leads to different single crystal shapes observed experimentally. Chain folding along the *a*-axis is recognized on the basis of the evidence from polymer decoration and lamellar microdeformation experiments. With decreasing crystallization temperature, spherulitic texture becomes dominant and an edge-on type of narrow ribbon-like lamellar orientation in the spherulites is increasingly distorted. The morphology of PEKK(T) obtained *via* solvent-induced crystallization by methylene chloride shows very small crystallites having a size less than 50 nm in three dimensions.

## Introduction

Poly(aryl ether ketone ketone)s (PEKKs) are the most common members of a new class of high-temperature, high-performance engineering thermoplastics possessing high potential in structural composite, fire retardant materials, and other specific applications. Their useful properties include high melting and glass transition temperatures, a wide range of attainable crystallinities, good chemical resistance, and low flammability. These properties are combined with good processability which allows them to be shaped into various forms such as molded parts, fibers, films, and coatings. Since these desirable macroscopic properties are directly related to the microscopic structure and morphology of each particular sample, we have recently initiated a series of detailed studies of the crystal structure and morphology of PEKKs. This work has been concerned with the examination of structure and structural changes with various crystallization conditions<sup>1–3</sup> and the determination of thin film morphological characteristics of the samples.

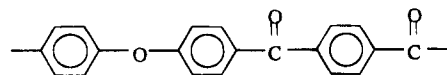
The crystalline morphology of the polymer is dependent on molecular weight, crystallization temperature (more precisely, supercooling), time, and preparation scheme. We have found that PEKK having all *p*-phenylene linkages [PEKK(T)] is an ideal candidate for the study of morphology under different crystallization conditions because PEKK(T) can be isothermally crystallized over a wide temperature range (*ca.* 200 °C). This is combined with the fact that the maximum crystallization rate of the polymer is slow enough to allow it to be quenched to temperatures below its glass transition temperature before crystallization occurs.

PEKK(T) shows polymorphism in its crystal structure, depending upon the crystallization conditions and crystallization methods.<sup>1,4–6</sup> The form I structure has a two-chain orthorhombic lattice with dimensions of *a* = 0.767 nm, *b* = 0.606 nm, and *c* = 1.008 nm which can be found when the samples are crystallized from the melt at low supercoolings. On the other hand, a two-chain orthorhombic lattice with dimensions of *a* = 0.417 nm, *b* = 1.134 nm, and *c* = 1.008 nm can be obtained *via* solvent-induced crystallization and cold crystallization from the glassy state and has been assigned as the form II structure.<sup>1,4–6</sup>

In this paper, we report our attempt to study the polycrystalline morphological dependence on crystallization methods and temperature *via* transmission electron microscopy (TEM) and electron diffraction (ED) experiments on PEKK(T) single crystals of both forms. The observed single crystal shapes can be explained by tilting of the *c*-axis in those crystals. The study in chain-folding behavior of PEKK crystals is carried out *via* polymer decoration and microdeformation methods.

## Experimental Section

**Materials and Samples.** Developmental grade PEKK(T) with all *p*-phenylene linkages was prepared from diphenyl ether and terephthalic acid in a two-step process by DuPont. Its chemical structure is



The number-average molecular weight of the samples is around 10 000 and the polydispersity is 3.

PEKK(T) thin films with a thickness ranging from 0.01 to 0.1 μm were prepared for TEM observations by casting a 0.1% (w/w) PEKK(T)–pentafluorophenol (PFP) solution onto carbon-coated glass slides. The solvent was evaporated in a vacuum oven, and the films were then stripped, floated onto the water

\* To whom correspondence should be addressed.

† Abstract published in *Advance ACS Abstracts*, November 15, 1995.

surface, and recovered using nickel grids. First, the samples were heated to *ca.* 20 °C above their equilibrium melting temperature (410 °C for PEKK(T)<sup>6</sup>) for several minutes under a dry nitrogen atmosphere. Then they were either quenched into liquid nitrogen to generate amorphous glassy films for the purpose of cold crystallization or rapidly cooled to a preset temperature for melt-crystallization experiments. For solvent-induced crystallization, the amorphous glassy films were exposed at room temperature in methylene chloride for 1 week. The PEKK(T) thin films were also shadowed by Pt and coated with carbon for TEM observations. For wide angle X-ray diffraction (WAXD) measurements, PEKK(T) films having a thickness of about 0.1 mm were prepared by solution casting 2% PEKK-PFP (w/w) at 80 °C. The solvent was then evaporated in a vacuum oven. The same thermal and crystallization procedures were applied to the samples as described earlier.

For the polymer decoration experiments, polyethylene (PE) was vaporized by heating under vacuum (typically,  $10^{-4}$ – $10^{-5}$  Torr) and then crystallized on the fold surface of PEKK(T) single lamellar crystals. In this process, thermally induced chain scission on PE occurs. During highly anisotropic decorating the PE crystal rods become oriented parallel to the fold direction on the PEKK(T) single crystals.<sup>7,8</sup> The number-average molecular weight of PE in this experiment is around 10 000, and the polydispersity is 1.1 before the chain scission. After decoration, the samples were shadowed by Pt and coated with carbon. They were then stripped, floated onto the water surface, and recovered using nickel grids for TEM observations.

For the microdeformation experiments, PEKK(T) thin films were also prepared by following the same procedure described previously. The samples were crystallized from the melt or the glassy state at low supercoolings (high crystallization temperatures) in order to obtain single lamellar crystals. They were stripped, floated onto the water surface, and recovered using Mylar films. The microdeformation of the PEKK(T) crystals was achieved through a uniaxial plastic deformation of Mylar substrate. A typical elongation is around 35%. After deformation, the samples were shadowed by Pt (the direction of shadowing was perpendicular to the drawing direction) and coated with carbon. The samples were then stripped by poly(acrylic acid) (PAA), floated onto the water surface to dissolve PAA, and recovered using copper grids for TEM observations.

**Instrumentation and Experiments.** PEKK(T) crystalline morphology and ED patterns were observed via a JEOL (1200 EX II) TEM using an accelerating voltage of 120 kV. A tilting stage was also used in ED experiments to determine the three-dimensional crystal unit cells. Calibration of the ED spacings was carried out using Au and TiCl<sub>3</sub> in a *d*-spacing range smaller than 0.384 nm, which is the largest spacing for TiCl<sub>3</sub>. Spacing values greater than 0.384 nm were calibrated by doubling the *d*-spacings of those reflections on the basis of their first-order reflections.

Reflection WAXD experiments were conducted through a Rigaku 12 kW rotating-anode generator (Cu K $\alpha$ ) with diffractometer. The X-ray beam was monochromatized using a graphite crystal. The  $2\theta$  angle region ranges between 5 and 35° with a scanning rate of 2°/min. The diffraction peak positions and widths observed from WAXD experiments were carefully calibrated through silicon crystals with known crystal sizes. A custom-built hot stage was set up on the diffractometer. The temperature control is better than  $\pm 1.5$  °C in the temperature range for this study. The scans were conducted at each isothermal crystallization temperature after complete crystallization of the PEKK(T) samples.

## Results and Discussion

**Polycrystalline Morphological Dependence on Crystallization Methods and Temperature.** Figure 1 shows polymorphism of PEKK(T) having all *p*-phenylene linkages obtained via different crystallization conditions and methods based on our WAXD observations.<sup>1</sup> It is evident that in certain temperature ranges of the melt and cold crystallizations both forms exist.

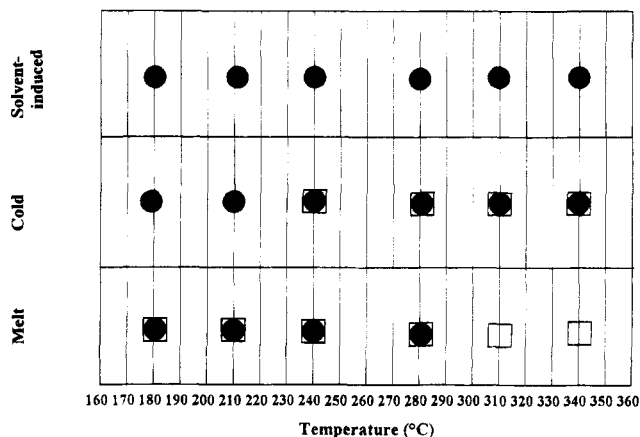


**Figure 1.** Phase formation maps of both form I (open squares) and form II (filled circles) at different temperatures from the melt, the glassy state, and solvent-induced crystallization.

For example, PEKK(T) samples crystallized from the melt exhibit a major formation on form I in the whole temperature range. However, a very minor population of the form II structure can be detected between  $T_g$  and 280 °C. On the other hand, the cold crystallization of PEKK(T) samples produces a major population of the form II structure at least up to 310 °C, although a very minor portion of the form I structure can also be found down to 240 °C. Above 310 °C, the ability of growing the form I structure is significantly enhanced.<sup>1</sup> It is known that form I is thermodynamically more stable than form II. The formation mechanisms of these two forms are not fully understood at this moment. We speculate that the ability to develop each of the form structures may be closely associated with the nucleation process and chain mobility during the crystallization.<sup>1,6</sup>

For melt-crystallized PEKK(T) in a wide crystallization temperature range between 160 and 360 °C, spherulitic morphology can usually be observed. At high supercoolings near the glass transition temperature, the nucleation density is relatively high and the crystal growth rate is mainly affected by the transport term due to a low chain mobility. Both effects lead to a random orientation, which deviates away from the edge-on lamellar orientation.<sup>9</sup> A typical morphology is shown in Figure 2 for PEKK(T) crystallized from the melt at 180 °C for 2 h. Poorly defined, indistinct lamellar layers with diffuse spherulitic boundaries have been found. An ED pattern is also included in this figure to study the crystal orientation in the spherulite. As analyzed by Lovinger *et al.*, the *b*-axis is along the radial direction of the spherulitic growth.<sup>9</sup> However, the *c*-axis is not exactly parallel to the film surface, as is required by the edge-on type of lamellae. When the supercooling is reduced, the size of the spherulites becomes increasingly larger. For example, in the case of PEKK(T) crystallized at 310 °C from the melt for 60 min (Figure 3), the size of spherulites is *ca.* 12  $\mu$ m on average due to the decreasing nucleation density and enhanced molecular mobility. A 38°-tilted ED pattern was taken from the layers of lamellae in the spherulite (included in Figure 3) consisting of the *110* and *111* reflections. This suggests that PEKK(T) thin films crystallized at high temperatures do not change the spherulitic growth orientation along the *b*-axis which is in the radial direction of the spherulites. The *c*-axis (chain direction in molecules) is tangential to the plane of the film, and the *a*-axis is tangential normal to the spherulitic plane, indicating that edge-on growth is preferred.



**Figure 2.** TEM observations of PEKK(T) spherulitic crystals grown from the melt at 180 °C for 2 h. An ED pattern is also included which is taken from the circled area in the figure and shown in correct orientation.

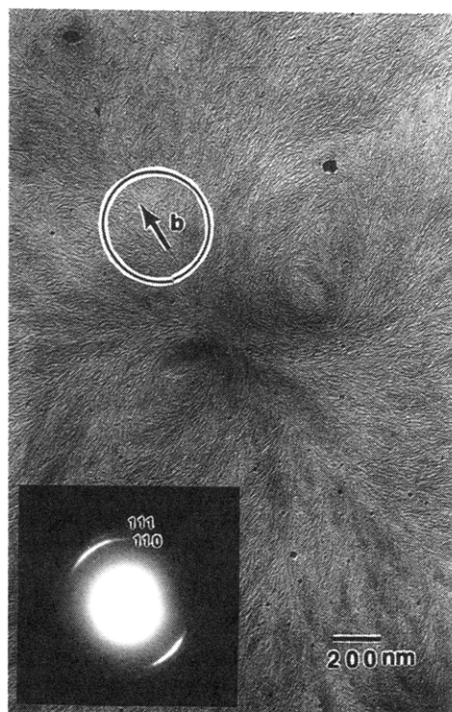


**Figure 3.** TEM observations of PEKK(T) spherulitic crystals grown from the melt at 310 °C for 60 min. The ED pattern originates from the circled area with a 38°-tilted angle and is shown in correct orientation.

On the basis of the spherulitic model in poly(aryl ether ether ketone) (PEEK) thin film first proposed by Lovinger *et al.*,<sup>9</sup> our ED results indicate that the spherulitic morphology in the PEKK(T) thin film also possesses a cylindrical arrangement at low supercoolings. When the supercooling is increased, these lamellar crystals become increasingly disordered in the cylindrical arrangement of the spherulites (*i.e.*, a more random lamellar orientation by changing the angle between the *c*-axis and the film surface away from 0°),

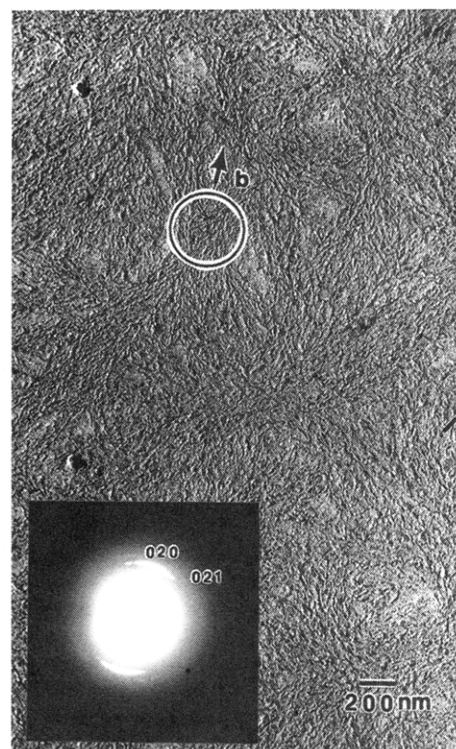


**Figure 4.** TEM observations of PEKK(T) spherulitic crystals grown from the glassy state at 310 °C for 60 min. The ED pattern originates from the circled area of the spherulite and is shown in correct orientation.

while the *b*-axis remains radial. Therefore, a rough surface texture for the spherulitic morphology is observed (Figure 2) as compared with the smooth surface texture on the spherulitic morphology crystallized at low supercoolings (Figure 3).

Spherulitic morphology consisting of narrow ribbon-like lamellae can also be observed in PEKK(T) crystallized from the glassy state at 310 °C for 60 min (Figure 4). The average size of the spherulites is *ca.* 0.5  $\mu\text{m}$ . An ED pattern is also included in Figure 4. On the basis of the relationship between the 020 reflection of form II and the lamellar orientation in the spherulites, we conclude that the *b*-axis of the unit cell in form II is also radial as in the form I spherulites. In general, however, the size of spherulites crystallized from the glassy state is smaller than that from the melt and a more random lamellar orientation of the *c*-axis with respect to the film surface is observed in cold crystallization.

Methylene chloride can strongly interact with PEKK(T) and induce significant swelling. The absorbed solvent plasticizes the amorphous PEKK(T) to a level at which the transformation of the amorphous phase to the lower free energy crystals is favored. This phenomenon is known as solvent-induced crystallization. The TEM observations of the crystal morphology *via* solvent-induced crystallization is shown in Figure 5. Very small crystallites with a typical size of less than 50 nm in three dimensions are observed. Unlike crystals grown from the melt or the glassy state, no narrow ribbon-like lamellae can be found in this case. As a result, we speculate that nucleation is strongly dominant during this crystallization and molecular mobility is very limited. An ED pattern obtained from this kind of morphology only shows reflection rings (Figure 5). This reveals the small crystallite sizes as well as random orientation of the crystals in this solvent-induced crystallization process.

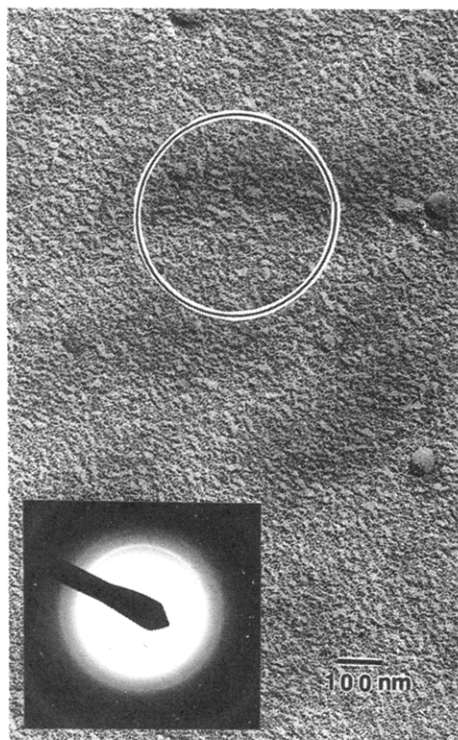


**Figure 5.** TEM observations of PEKK(T) crystals obtained *via* solvent-induced crystallization. An ED pattern originating from the circled area in the figure is also included.

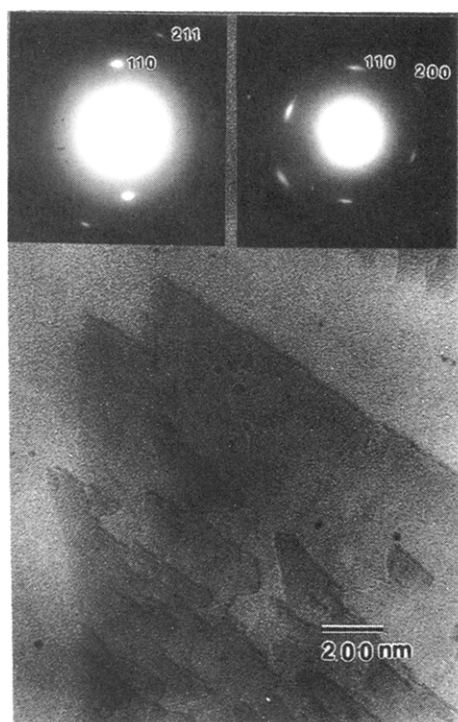


**Figure 6.** TEM observations of PEKK(T) form I single lamellar morphology grown from the melt at 360 °C for 20 h. Untilted and 60°-tilted ED patterns originating from the circled area of the micrograph are shown in correct orientation, and they are along the  $[1\bar{1}1]$  and  $[00l]$  zones, respectively.

**Single Lamellar Crystals of Both Forms.** At a high crystallization temperature of 360 °C, micrometer-size single lamellar crystals with faceted linear edges can be observed in the PEKK(T) thin film samples, as shown in Figure 6. Furthermore, the single crystals exhibit a lozenge shape. In all the cases, only a part of the lamellar crystals can be seen on the sample surfaces.

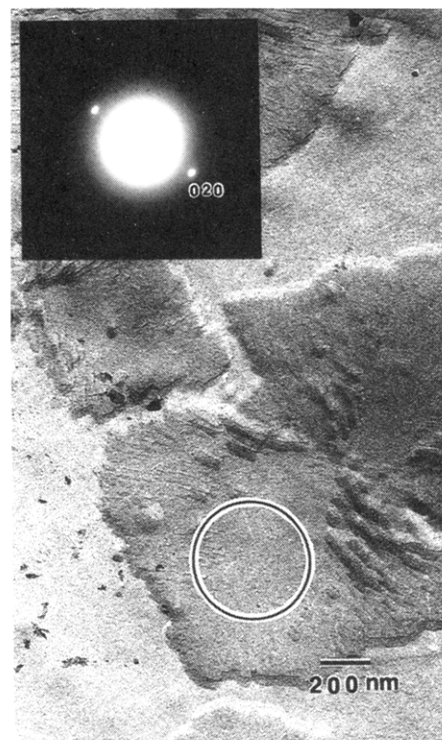


**Figure 7.** TEM observations of PEKK(T) form II single lamellar morphology grown from the glassy state at 360 °C for 20 h. The ED pattern originates from the circled area of the micrograph and is shown in correct orientation.

The ED pattern of the single lamellar crystals indicates the form I unit cell (included in Figure 6). The electron beam is parallel to the  $[1\bar{1}1]$  zone since  $110$  and  $211$  reflections are observed. This indicates that the  $c$ -axis of the lamellar crystals is not parallel to the electron beam. After a tilting angle of *ca.* 60°, an ED pattern with the  $[00l]$  zone can be found (also included in Figure 6). A similar observation of such tilting of the molecular chains to the lamellar normal in the PEEK crystals has been recently reported by Lovinger *et al.*<sup>10</sup> Interestingly, micrometer-size faceted single crystals can also be found in form II as the sample crystallized from the glassy state at 360 °C (Figure 7). However, the single crystal shape in this case is symmetric. An ED pattern of the single crystals is also included in Figure 7, and it only shows  $b$ -axis reflections of  $020$  and  $040$ . Similar to the form I single crystals, the  $c$ -axis of form II single crystals is also not parallel to the electron beam. Through the tilting stage, ED patterns along the  $[00l]$  zone can be obtained. A roughly estimated  $40 \pm 5^\circ$  of molecular inclination to the substrate normal along the  $b$ -axis can be found.

To investigate the relationship between the unit cell orientation and the shape observed in the single crystals, we have carried out detailed crystallographic analysis for the single lamellar crystal orientation in these samples. On the basis of the ED results shown in Figure 6, the observed  $[1\bar{1}1]$  zone indicates that the angle between the electron beam (which is perpendicular to the substrate) and the  $c$ -axis is  $65^\circ$  (this angle is redetermined compared with that previously reported).<sup>1</sup> The rotating axis is found to be along the  $110$  direction. If one views the single crystal parallel to the  $c$ -axis, the edge planes should thus be  $\{310\}$  planes, as shown in Figure 8a. The two angles formed by the faceted edges are  $134.2$  and  $45.8^\circ$ , respectively. After the  $65^\circ$  rotation along the  $110$  direction, the projections of the  $a$ - and  $b$ -axes in the unit cell are as shown in Figure 8b. The



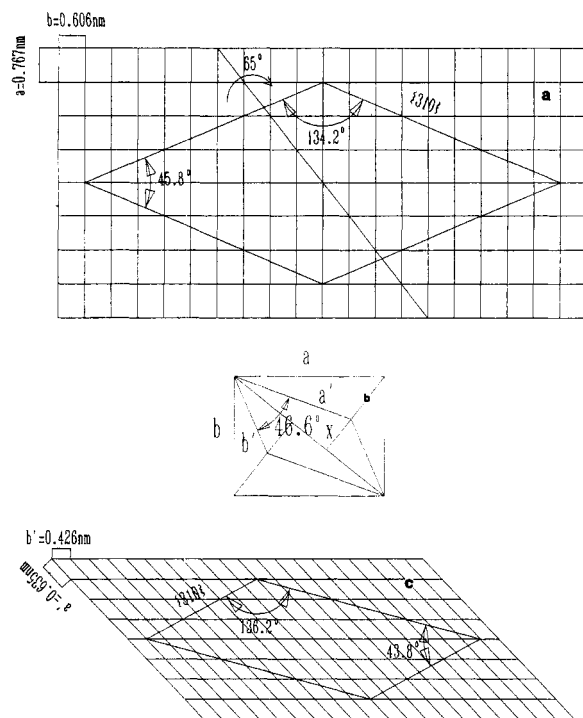


**Figure 8.** Set of schematic illustrations of PEKK(T) form I single lamellar orientation: (a) viewing direction parallel to the  $c$ -axis; (b) projections of  $a$ - and  $b$ -axes after rotation along  $[110]$  for  $65^\circ$ ; (c) expected single crystal shape that should be observed experimentally.

$a'$ -axis length is thus 0.635 nm and that of the  $b'$ -axis is 0.426 nm. The value of  $x = 0.201$  nm is the distance between the corner of the unit cell and the  $(110)$  plane. This rotation leads to the  $[1\bar{1}\bar{1}]$  zone, and the single crystal should possess the shape of Figure 8c. The projections of these two angles formed by the faceted edges are thus  $136.2$  and  $43.8^\circ$ , respectively. Indeed, the experimentally observed single lamellar crystals fit well as these predicted ones. The asymmetrical shape of the single crystals shown in Figure 8c is difficult to observe in TEM results since only a part of the single crystals can be seen (see Figure 6 as well as Figure 4 in ref 1). This may also be an indication that the lamellar fold surface normal is not perpendicular to the substrate. Similar analysis can also be conducted for the form II single crystals. Figure 9a illustrates the form II single crystal when the viewing direction is parallel to the  $c$ -axis. On the basis of the ED pattern in Figure 7, the faceted edge planes are  $\{120\}$  planes and the two angles between the edge planes are  $107.3$  and  $72.7^\circ$ , respectively. Since the rotating axis is along the  $b$ -axis and the rotating angle is  $40^\circ$ , Figure 9b indicated that the  $a'$ -axis is 0.319 nm after the rotation. This leads to an expected symmetric single crystal with two angles of  $121.3$  and  $58.7^\circ$ , as shown in Figure 9c. Again, it fits our experimental observation, as shown in Figure 7.

#### Chain-Folding Behavior of PEKK(T) Crystals.

In order to study the chain-folding behavior of PEKK(T) lamellar crystals, polymer decoration on the fold surface of PEKK(T) single crystals has been conducted. The method based on the vaporization and condensation-crystallization of polymer fragments (for example, PE) as decorating materials was first proposed by Wittmann and Lotz in the early 1980s to study the single crystal surface topography of polymers.<sup>7,8</sup> On the basis of the orientation of elongated crystal rods on the surface of polymer single crystals, preferential orienta-

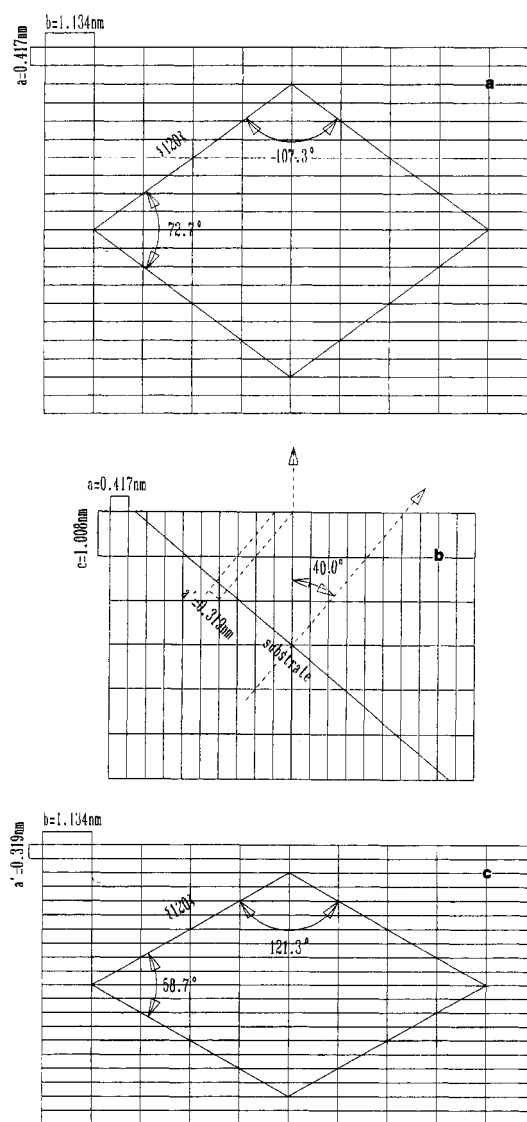


**Figure 9.** Set of schematic illustrations of PEKK(T) form II single lamellar orientation: (a) viewing direction parallel to the  $c$ -axis; (b) projections of the  $a$ -axis after the rotation along the  $b$ -axis for  $40^\circ$ ; (c) expected single crystal shape that should be observed experimentally.

tion of polymer folding can be determined. Figure 10 shows a TEM micrograph of PEKK(T) form I single crystals after PE decoration (the single crystals have been bounded by solid lines). It is interesting to observe that the narrow rod PE crystals tend to orient along the  $b$ -axis direction of the single crystals. No indication of the sectorization for this single crystal is observed. On the basis of the orientation of PE crystal rods, we suggest that the fold orientation of the single crystals is along the  $a$ -axis direction, which is perpendicular to the crystal growth direction. However, we cannot obtain PE crystal diffraction from the decorated PEKK(T) single crystals regardless of substantial effort. This may be attributed to the tilted lamellar surface of the PEKK(T) with respect to the  $c$ -axis. Therefore, the  $110$  and/or  $200$  electron diffractions that are commonly observed in PE single crystals cannot be observed. Similar to PEKK(T) form I single crystals, the narrow rod PE crystals tend to orient along the  $b$ -axis direction for PEKK(T) form II single crystals, as shown in Figure 11. This suggests form I and form II crystals may possess the same fold orientation (i.e., along the  $a$ -axis direction). It is known that the lateral growth shape observed in a single lamellar crystal should be bounded

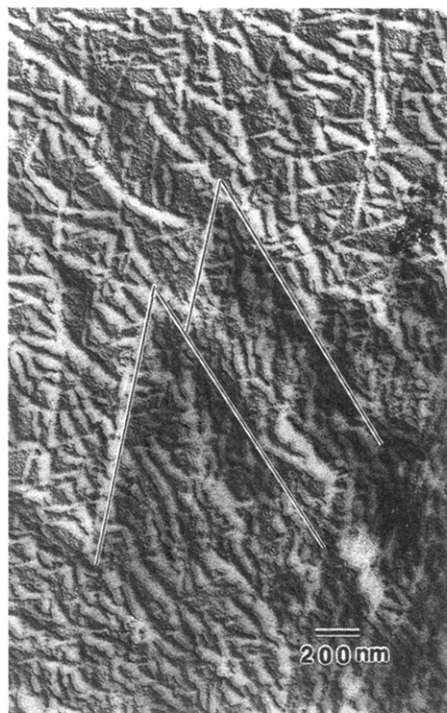


**Figure 10.** TEM micrograph of PEKK(T) form I single lamellar crystals decorated with PE vapor.

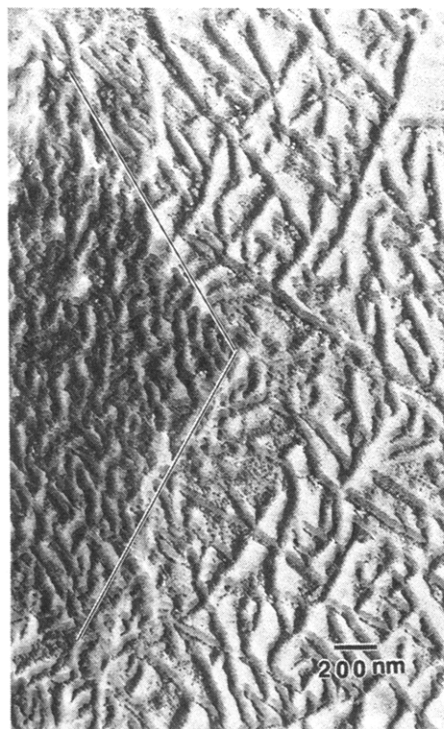


**Figure 11.** TEM micrograph of PEKK(T) form II single lamellar crystals decorated with PE vapor.

by the slowest growing planes. Nevertheless, how to accommodate this folding direction to the formation of the  $\{310\}$  or  $\{120\}$  edge planes in both forms needs further investigation.

Microdeformation in PEKK(T) single lamellar crystals is also examined to identify the folding behavior. Figure 12 shows a typical TEM micrograph of a deformed PEKK(T) form I single crystal in which the direction of imposed strain is along the  $b$ -axis of the single crystal. Periodically separated transverse microcracks which are aligned along the  $a$ -axis direction develop a response

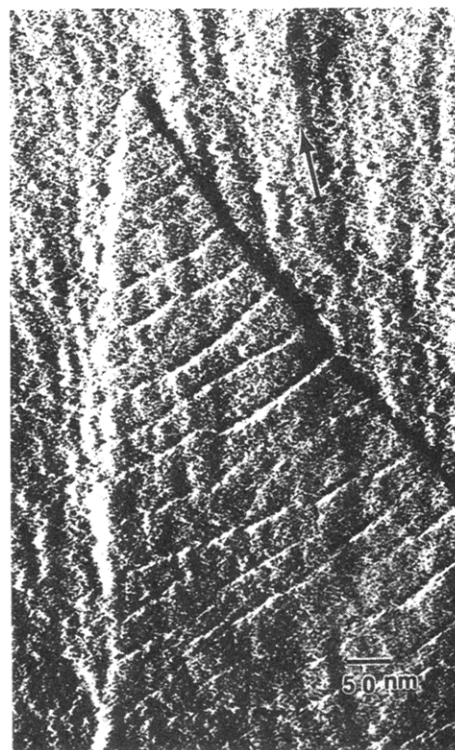


**Figure 12.** TEM micrograph of microdeformation of PEKK(T) form I single lamellar crystals under an elongation of 35% along the arrow direction. The direction of deformation is along the  $b$ -axis.

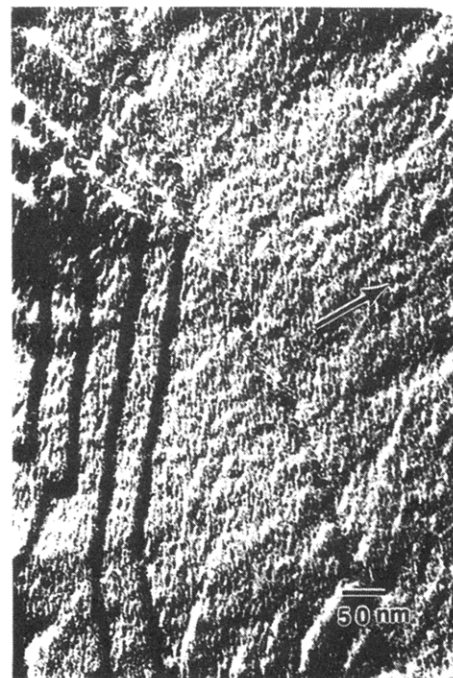


**Figure 13.** TEM micrograph of microdeformation of PEKK(T) form I single lamellar crystals under an elongation of 35% along the arrow direction. The direction of deformation is along the  $a$ -axis.

to the imposed strain and can be observed for the single crystal. Furthermore, no microfibril has been found within the microcracks. It may thus be an indication that the fold orientation is not along the  $b$ -axis direction. On the other hand, no microcrack can be found when the direction of imposed strain is along the  $a$ -axis of the single crystal, as shown in Figure 13. This manifests that deformation for PEKK(T) single crystals is much

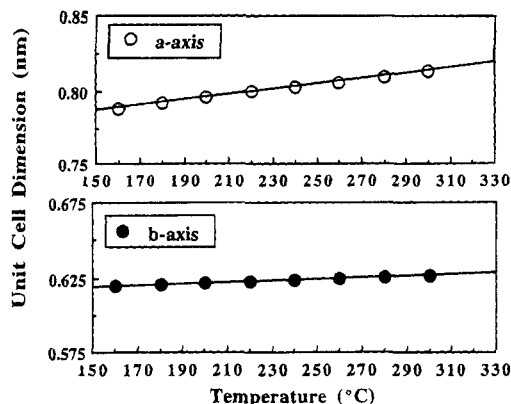


**Figure 14.** Unit cell dimension changes with temperature for form I crystals along the *a*-axis (a) and *b*-axis (b).

easier along the *b*-axis direction than along the *a*-axis. In fact, over 100 electron micrographs have been taken and, regardless of the percentage of the elongation, the crystals cannot be deformed along the *a*-axis. Although poor adhesion between the Mylar film surfaces and crystal fold surfaces may exist, the anisotropic response to the imposed strain supports the conclusion of the *a*-axis fold orientation for PEKK(T) crystals determined *via* the polymer decoration method. It is known that a lattice strain can be introduced *via* the chain fold orientation. Thermal expansion along the fold direction must thus be greater than that in other directions due to the lattice strain, particularly in a relatively rigid polymer such as PEKK(T). The temperature dependence of the unit cell dimensions for PEKK(T) form I crystals has been determined *via* WAXD experiments and is shown in Figure 14. A slightly dimensional increase with temperature along the *b*-axis is found. However, the *a*-axis dimension is relatively sensitive to temperature. The linear coefficient of thermal expansion along the *a*-axis is about 3 times higher than that of the *b*-axis. Similar results can also be found in PEKK(T) form II crystals (Figure 15).

## Conclusions

The thin film crystalline morphology of PEKK(T) is strongly dependent on the crystallization conditions and methods. At low supercoolings, micrometer-size faceted single lamellar crystals can be grown either from the melt or from the glassy state. The {310} and {120} planes are the faceted edge planes for form I and form II, respectively. Relationships between the tilting *c*-axis and single crystal shape have been established on the basis of the crystallographic analyses. The morphology of PEKK(T) crystals crystallized *via* solvent-induced

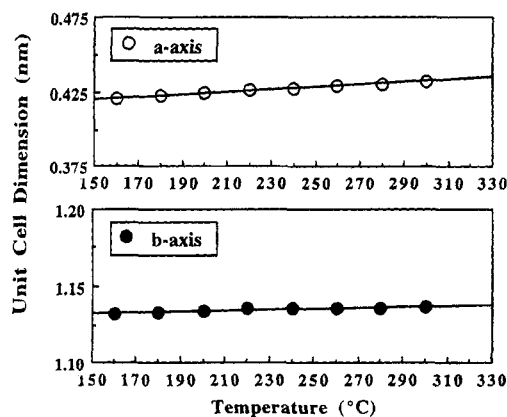


**Figure 15.** Unit cell dimension changes with temperature for form II crystals along the *a*-axis (a) and *b*-axis (b).

crystallization by methylene chloride does not show narrow ribbon-like lamellae, and the crystallite size is smaller than 50 nm. The folding behavior for PEKK(T) crystals is studied through polymer decoration experiments. The fold orientation is determined to be along the *a*-axis direction of PEKK(T) single crystals. The microdeformation method provides indirect but consistent results with this fold orientation. The *a*-axis dimension is more sensitive to temperature than the *b*-axis dimension. One of the reasons is due to the lattice strain along the folding direction.

**Acknowledgment.** This research was supported by SZDCs Presidential Young Investigator Award from the National Science Foundation (DMR 91-57738) and the industrial matching funding from DuPont.

## References and Notes

- (1) Ho, R. M.; Cheng, S. Z. D.; Hsiao, B. S.; Gardner, K. H. *Macromolecules* **1994**, *27*, 2136.
- (2) Ho, R. M.; Cheng, S. Z. D.; Fisher, H. P.; Eby, R. K.; Hsiao, B. S.; Gardner, K. H. *Macromolecules* **1994**, *27*, 5787.
- (3) Ho, R. M.; Cheng, S. Z. D.; Hsiao, B. S.; Gardner, K. H. *Macromolecules* **1995**, *28*, 1938.
- (4) Avakian, P.; Gardner, K. H.; Matheson, R. R. *J. Polym. Sci., Polym. Symp.* **1990**, *28*, 243.
- (5) Blundell, D. J.; Newton, A. B. *Polymer* **1991**, *32*, 308.
- (6) Gardner, K. H.; Hsiao, B. S.; Matheson, R. R.; Wood, B. A. *Polymer* **1992**, *33*, 2484.
- (7) Wittmann, J.-C.; Lotz, B. *Makromol. Chem., Rapid Commun.* **1982**, *3*, 733.
- (8) Wittmann, J.-C.; Lotz, B. *J. Polym. Sci., Polym. Phys. Ed.* **1985**, *23*, 205.
- (9) Lovinger, A. J.; Davis, D. D. *J. Appl. Phys.* **1985**, *58*, 2843.
- (10) Lovinger, A. J.; Hudson, S. D.; Davis, D. D. *Macromolecules* **1992**, *25*, 1752.

MA950686T